JOURNAL OF MATERIALS SCIENCE 22 (1987) 2175–2180

Strength and elongation of multifilamentary Nb_3Sn superconducting composite materials with small amounts of Nb_3Sn compound

SHOJIRO OCHIAI, KOZO OSAMURA
Department of Metallurgy, Kyoto University, Sakyo-ku, Kyoto 606, Japan

In order to describe the tensile strength and elongation to failure of multifilamentary Nb_3Sn superconducting composite materials with small amounts of Nb_3Sn showing multiple fracture, approximate calculation methods are proposed. In the proposed calculation methods, the concept of shear-lag analysis and the plastic instability approach for metallic composites are employed. The experimental results are fairly well described by the present calculation methods.

1. Introduction
In our former work [1], it was found that Nb_3Sn multifilamentary bronze-processed superconducting composite materials consisting of Nb_3Sn compound, niobium filaments, Cu–Sn matrix, niobium barrier and copper as a stabilizer show two types of fracture mode, depending on the volume fraction of Nb_3Sn compound. When the fraction of Nb_3Sn is small, the drop of load-bearing capacity due to fracture of Nb_3Sn can be compensated mainly by strain-hardening of the ductile constituents of niobium, Cu–Sn and copper. This results in a Type I fracture mode, characterized by high elongation to failure of composites as a whole and multiple fracture of the compound. On the other hand, when the fraction of Nb_3Sn is large, the fracture of one region of Nb_3Sn causes fracture of neighbouring Nb_3Sn regions one after another. This results in a Type II fracture mode, characterized by a brittle fracture mode of composites as a whole with very low elongation to fracture, being nearly equal to the fracture strain of the Nb_3Sn compound, and no multiple fracture of the compound. The dependency of fracture mode on volume fraction of Nb_3Sn compound can be explained by the Kelly–Tyson model [2] as shown in our former work [1].

The Type II fracture mode is analogous to that of fibre-reinforced metals, which has been studied in detail [3–10]. On the other hand, the Type I fracture mode has not been studied in detail up to date. The aim of the present paper is to describe the strength and elongation of multifilamentary Nb_3Sn superconducting composite materials which have small volume fractions of Nb_3Sn and therefore show multiple fracture of Nb_3Sn.

2. Experimental results
The analysis of strength and elongation to failure was carried out for multifilamentary composite wires consisting of a total of 745 niobium filaments embedded in Cu–Sn matrix, niobium barrier and copper as stabilizer, where the overall diameter was 2.6 mm. As the microstructure and tensile behaviour of specimens before and after annealing at 973 and 1073 K up to 1730 ksec has been studied in detail in our former works, in which the specimens analysed in the present work were named as S3 [1], the strength and elongation to failure will be analysed using the data presented in our former work [1].

3. Modelling and calculation method
In the present work, the niobium, Nb_3Sn, Cu–Sn and copper are denoted 1 to 4, respectively, and the interfaces between niobium and Nb_3Sn and that between Nb_3Sn and Cu–Sn as 1–2 and 2–3, respectively.

3.1. Modelling of composites
In all specimens investigated, the Nb_3Sn compound showed multiple fracture as typically shown in Fig. 1. In order to formulate the distribution of tensile stress and strain, one should beforehand model how the Nb_3Sn compound is broken. In this point, one can hit on two extreme cases A and B, as shown in Fig. 2, under the approximation that the length of segmented Nb_3Sn compound, l, is the same in each case. In Case A, the fracture of Nb_3Sn occurs homogeneously on a macroscopic scale. On the other hand, in Case B the fracture of Nb_3Sn occurs at the same cross-sections.

In Case A, the strain of ductile components of niobium, Cu–Sn and copper could be approximated to have the same strain $\bar{\varepsilon}$ (= strain of composite as a whole) at any cross-section, and also the contribution of stress of segmented Nb_3Sn ($= \bar{\sigma}_2 V_2$ where $\bar{\sigma}_2$ is the average stress of Nb_3Sn) to that of the composite is the same in each cross-section. Namely, taking x as the distance from one fracture end of Nb_3Sn, where $x = 0$ and l correspond to one fracture end and another one, respectively, as shown in Fig. 2, the values of $\bar{\varepsilon}$ and $\bar{\sigma}_2$ are independent of x, to a first approximation.

On the other hand, in Case B, the strain of ductile components is highest in the cross-sections where the Nb_3Sn is broken and it decreases with increasing x up

0022–2461/87 $03.00 + .12

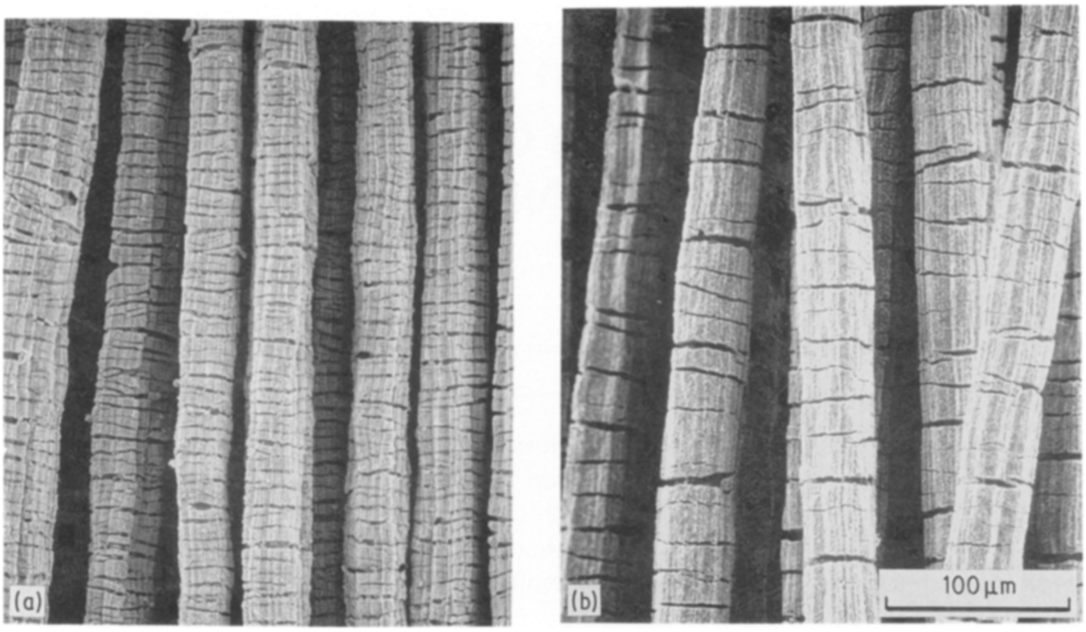

Figure 1 Multiple fracture of Nb_3Sn compound after fracture of composites as a whole in specimens annealed at (a) 973 K for 432 ksec and (b) 1073 K for 1730 ksec. The copper stabilizer, niobium barrier and a portion of the Cu–Sn matrix were removed by chemical etching after the tensile test.

to $x = l/2$ where the strain of ductile components is lowest, while the contribution of stress of Nb_3Sn to that of the composite is zero at $x = 0$ but increases with increasing x, reaching a maximum at $x = l/2$. The strain of the composite as a whole, $\bar{\varepsilon}$, is given by the average of the strain from $x = 0$ to l.

3.2. Calculation method of strength and elongation for Case (A)

In the present work, the triaxial stresses arising from the difference of mechanical properties among the constituents and from the fracture of Nb_3Sn compound are neglected as a first approximation, and the stress in each component in the longitudinal direction will be calculated.

For ductile components, the relation of true tensile stress σ to true tensile strain ε can be approximately expressed by

$$\sigma = E\varepsilon \qquad \text{for } \varepsilon \leqq \varepsilon_y \qquad (1)$$

$$\sigma = [a + b(\varepsilon - \varepsilon_y)]^n \qquad \text{for } \varepsilon > \varepsilon_y \qquad (2)$$

where E is the Young's modulus, ε_y is the tensile yield strain given by σ_y/E where σ_y is the tensile yield stress,

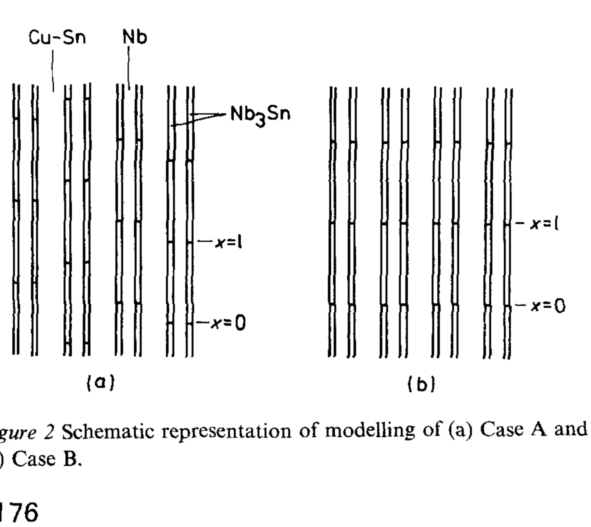

Figure 2 Schematic representation of modelling of (a) Case A and (b) Case B.

and a, b and n are constants which can be determined by solving Equations 3 to 5 below, using known values of yield stress σ_y, tensile strength σ_u and normal elongation to failure e_u, which is converted to true strain ε_u by $\varepsilon_u = \ln(1 + e_u)$:

$$\sigma_y = a^n \qquad (3)$$

$$\varepsilon_u = \frac{nb - a}{b} + \varepsilon_y \qquad (4)$$

$$\sigma_u = (nb)^n \exp(-\varepsilon_u) \qquad (5)$$

The normal stress of composites σ_c at high strain for Case A is given by

$$\sigma_c = \{[a_1 + b_1(\bar{\varepsilon} - \varepsilon_{y1})]^{n_1} V_1 + [a_3 + b_3(\bar{\varepsilon} - \varepsilon_{y3})]^{n_3} V_3 + [a_4 + b_4(\bar{\varepsilon} - \varepsilon_{y4})]^{n_4} V_4\} \exp(-\bar{\varepsilon}) + \bar{\sigma}_2 V_2 \qquad (6)$$

The value of $\bar{\sigma}_2$ can be inferred in the following manner. The stress can be transferred to segmented Nb_3Sn through Nb–Nb_3Sn and Nb_3Sn–(Cu–Sn) interfaces. Picking up the element consisting of an inner core of niobium filament with a diameter of d_1, an outer sleeve of Cu–Sn with an inner diameter of d_{1+2} and an outer diameter of d_{1+2+3}, and Nb_3Sn between niobium and Cu–Sn, as shown in Fig. 3, the stress of Nb_3Sn, σ_2, at position x is given by

$$A_2 \frac{d\sigma_2(x)}{dx} = \pi d_1 \tau_{1-2}(x) + \pi d_{1+2} \tau_{2-3}(x) \qquad (7)$$

where A_2 is the area of Nb_3Sn in the element, and τ_{1-2} and τ_{2-3} are the shear stresses exerted at Nb–Nb_3Sn and Nb_3Sn–(Cu–Sn) interfaces, respectively. As the bonding strengths between niobium and Nb_3Sn and between Nb_3Sn and Cu–Sn are high enough to suppress debonding at the respective interface, as ascertained with SEM observation, the shear stress at the former interface is determined by the shear stress of niobium and that at the latter interface by the shear

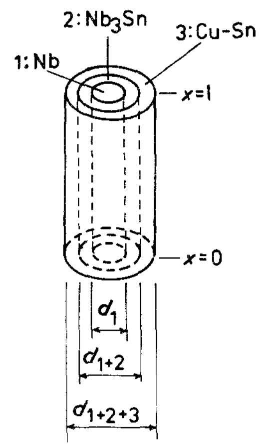

Figure 3 Schematic representation of an element with a length l, composed of (1) niobium filament, (2) Nb_3Sn compound and (3) Cu–Sn matrix.

stress of Cu–Sn. Substituting $\sigma = 2\tau$ where τ is the shear stress and $\varepsilon = \gamma/2$ where γ is the shear strain into Equation 1, and considering the yield phenomenon in shear, we have

$$\tau = G\gamma \qquad \text{for } \gamma \leqq \gamma_y \quad (8)$$

$$\tau = \frac{1}{2}\left[a + \frac{b}{2}(\gamma - \gamma_y)\right]^n \qquad \text{for } \gamma \geqq \gamma_y \quad (9)$$

In order to employ Equations 8 and 9, we should estimate γ.

As the strain $\bar{\varepsilon}$ is large enough compared to the strain of Nb_3Sn, the difference in displacement between niobium and Nb_3Sn, ΔU_{1-2}, and that between Nb_3Sn and Cu–Sn, ΔU_{2-3}, are approximately given by

$$\Delta U_{1-2} = \Delta U_{2-3} = \bar{\varepsilon}\left(\frac{l}{2} - x\right) \quad (10)$$

In order to estimate γ by using ΔU given by Equation 10, we apply the Dow's approximation [11]. Defining c_1 and c_3 as the distances of the centroids of niobium and Cu–Sn from the Nb–Nb_3Sn and Nb_3Sn–(Cu–Sn) interfaces, respectively, the shear strain between niobium and Nb_3Sn, γ_{1-2}, and that between Nb_3Sn and Cu–Sn, γ_{2-3}, are given by

$$\gamma_{1-2} = \frac{\Delta U_{1-2}}{c_1} = \bar{\varepsilon}\,\frac{(l/2) - x}{c_1} \quad (11)$$

$$\gamma_{2-3} = \frac{\Delta U_{2-3}}{c_3} = \bar{\varepsilon}\,\frac{(l/2) - x}{c_3} \quad (12)$$

$$c_1 = \frac{d_1}{2} - \frac{2^{1/2}}{4} d_1 \quad (13)$$

$$c_3 = \left(\frac{d_{1+2}^2 + d_{1+2+3}^2}{8}\right)^{1/2} - \frac{d_{1+2}}{2} \quad (14)$$

Taking $y = (l/2) - x$, the shear stress in niobium and that in Cu–Sn are lower than the respective shear yield stress for $0 \leqq y \leqq y_1$ and $0 \leqq y \leqq y_3$, respectively, where y_1 and y_3 are given by

$$y_1 = c_1\gamma_{y_1}/\bar{\varepsilon} \quad (15)$$

$$y_3 = c_3\gamma_{y_3}/\bar{\varepsilon} \quad (16)$$

respectively. Combining Equations 8 to 16, we have τ_{1-2} and τ_{2-3} as a function of y (or x) and then we have σ_2 at position y by integrating Equation 7. The results are summarized as follows.

When $y_1 \geqq y_3$, namely $c_1\gamma_{y_1} \geqq c_3\gamma_{y_3}$,

$$\sigma_2 = \frac{1}{A_2}\left(\frac{\pi d_1 G_1 y^2 \gamma_{y_1}}{2y_1} + \frac{\pi d_{1+2} G_3 y^2 \gamma_{y_3}}{2y_3}\right) \qquad \text{for } y \leqq y_1, y_3 \quad (17)$$

$$\begin{aligned}\sigma_2 = \frac{1}{A_2}\Bigg\{&\frac{\pi d_1 G_1 y^2 \gamma_{y_1}}{2y_1} + \frac{\pi d_{1+2} G_3 y_3 \gamma_{y_3}}{2}\\ &+ \pi d_{1+2}\left\{\left[a_3 + \frac{b_3\gamma_{y_3}}{2}\left(\frac{y}{y_3} - 1\right)\right]^{n_3+1}\right.\\ &\left.- a_3^{n_3+1}\right\}\Bigg/\left[2(n_3 + 1)\frac{b_3\gamma_{y_3}}{2y_3}\right]\Bigg\}\end{aligned}$$

$$\text{for } y_3 \leqq y \leqq y_1 \quad (18)$$

$$\begin{aligned}\sigma_2 = \frac{1}{A_2}\Bigg\{&\frac{\pi d_1 G_1 y_1 \gamma_{y_1}}{2} + \frac{\pi d_{1+2} G_3 y_3 \gamma_{y_3}}{2}\\ &+ \pi d_1\left\{\left[a_1 + \frac{b_1\gamma_{y_1}}{2}\left(\frac{y}{y_1} - 1\right)\right]^{n_1+1}\right.\\ &\left.- a_1^{n_1+1}\right\}\Bigg/\left[2(n_1 + 1)\frac{b_1\gamma_{y_1}}{2y_1}\right]\\ &+ \pi d_{1+2}\left\{\left[a_3 + \frac{b_3\gamma_{y_3}}{2}\left(\frac{y}{y_3} - 1\right)\right]^{n_3+1}\right.\\ &\left.- a_3^{n_3+1}\right\}\Bigg/\left[2(n_3 + 1)\frac{b_3\gamma_{y_3}}{2y_3}\right]\Bigg\}\end{aligned}$$

$$\text{for } y \geqq y_1, y_3 \quad (19)$$

When $y_1 < y_3$, namely $c_1\gamma_{y_1} < c_3\gamma_{y_3}$, σ_2 is given by Equations 17 and 19 for $y \leqq y_1, y_3$, and $y \geqq y_1, y_3$, respectively. For $y_3 \geqq y \geqq y_1$, it is given by

$$\begin{aligned}\sigma_2 = \frac{1}{A_2}\Bigg(&\frac{\pi d_1 G_1 y_1 \gamma_{y_1}}{2} + \frac{\pi d_{1+2} G_3 y^2 \gamma_{y_3}}{2y_3}\\ &+ \pi d_1\left\{\left[a_1 + \frac{b_1\gamma_{y_1}}{2}\left(\frac{y}{y_1} - 1\right)\right]^{n_1+1}\right.\\ &\left.- a_1^{n_1+1}\right\}\Bigg/\left[2(n_1 + 1)\frac{b_1\gamma_{y_1}}{2y_1}\right]\Bigg)\end{aligned}$$

$$\text{for } y_1 \leqq y \leqq y_3 \quad (20)$$

Using Equations 17 to 20, the average stress of Nb_3Sn for both cases of $y_1 \geqq y_3$ and $y_1 \leqq y_3$ is given by

$$\begin{aligned}\bar{\sigma}_2 = \frac{\int_0^{l/2}\sigma_2\,\mathrm{d}y}{(l/2)} = \frac{2\pi}{lA_2}\Bigg\{&d_1\left(\frac{G_1 y_1^2\gamma_{y_1}}{6} + \frac{G_1 y_1\gamma_{y_1}[(l/2) - y_1]}{2}\right)\\ &+ d_{1+2}\left(\frac{G_3 y_3^2\gamma_{y_1}}{6} + \frac{G_3 y_3\gamma_{y_3}[(l/2) - y_3]}{2}\right)\\ &- d_1 a_1^{n_1+1}\frac{[(l/2) - y_1]}{2(n_1 + 1)(b_1\gamma_{y_1}/2y_1)}\\ &- d_{1+2} a_3^{n_3+1}\frac{[(l/2) - y_3]}{2(n_3 + 1)(b_3\gamma_{y_3}/2y_3)}\end{aligned}$$

$$+ d_1 \left\{ \left[a_1 + \frac{b_1 \gamma_{y_1}}{2} \left(\frac{l}{2y_1} - 1 \right) \right]^{n_1+2} - a_1^{n_1+2} \right\} \Bigg/ \left[2(n_1 + 1)(n_1 + 2) \left(\frac{b_1 \gamma_{y_1}}{2y_1} \right)^2 \right]$$

$$+ d_{1+2} \left\{ \left[a_3 + \frac{b_3 \gamma_{y_3}}{2} \left(\frac{l}{2y_3} - 1 \right) \right]^{n_3+2} - a_3^{n_3+2} \right\} \Bigg/ \left[2(n_3 + 1)(n_3 + 2) \left(\frac{b_3 \gamma_{y_3}}{2y_3} \right)^2 \right] \Bigg\} \quad (21)$$

As y_1 and y_3 are a function of $\bar{\varepsilon}$, the value of σ_c given by Equation 6 is a function of $\bar{\varepsilon}$.

In the next step, we deduce the load-bearing capacity of composites for Case A. According to Kelly and Tyson, who investigated tungsten fibre-reinforced copper [2], the strength of composites with a small volume fraction of fibre, in which multiple fracture of fibres is observed, is given by $\sigma_{mu} V_m$ where σ_{mu} is the tensile strength of the ductile matrix and V_m is the volume fraction of matrix. This suggests that the strength of such composites is determined by the load-bearing capacity of the ductile constituent, so that the contribution of segmented fibres to the strength of the composite is small. In our specimens the average length of segmented Nb_3Sn was very small, which allows necking of composites as a whole. With these in mind, the load-bearing capacity of the present composites can be deduced by calculating the load-bearing capacity of the ductile components. The load-bearing capacity of a ductile material can be given as the normal stress at which strain-hardening becomes unable to compensate for the reduction in area. This idea can be applied also for composites consisting of ductile components as shown by Mileiko [12], Garmong and Thompson [13] and Ochiai and Murakami [14]. In the present composites, the stress carried by ductile components, $\sigma_{c,d}$, at strain ε_d without Nb_3Sn is given by

$$\sigma_{c,d} = \{[a_1 + b_1(\varepsilon_d - \varepsilon_{y_1})]^{n_1} V_1 + [a_3 + b_3(\varepsilon_d - \varepsilon_{y_3})]^{n_3} V_3 + [a_4 + b_4(\varepsilon_d - \varepsilon_{y_4})]^{n_4} V_4\} \exp(-\varepsilon_d) \quad (22)$$

on the basis of the cross-sectional area of the composite as a whole. Differentiating Equation 22 with respect to ε_d, we can determine the value of ε_d at which $\sigma_{c,d}$ reaches a maximum and then the maximum value of $\sigma_{c,d}$.

Noting the maximum value of $\sigma_{c,d}$ as $\sigma_{c,max}$, which is the load-bearing capacity of the composite as a whole, we can calculate $\bar{\varepsilon}$ by equating $\sigma_c = \sigma_{c,max}$ in Equation 6.

3.3. Calculation method of strength and elongation for Case B

In Case A, the load at any cross-section is *a priori* assumed to be the same due to homogeneous fracture of Nb_3Sn. On the other hand, in Case B the equality of load at any cross-section should be formulated.

In Case B, the strain in the x direction of the composite is dependent on x. Assuming that the strain in the x direction is the same in the ductile components, the normal stress at position x is given by

$$\sigma_c = (\{a_1 + b_1[\varepsilon(x) - \varepsilon_{y_1}]\}^{n_1} V_1 + \{a_3 + b_3[\varepsilon(x) - \varepsilon_{y_3}]\}^{n_3} V_3 + \{a_4 + b_4[\varepsilon(x) - \varepsilon_{y_4}]\}^{n_4} V_4) \exp[-\varepsilon(x)] + \sigma_2(x) V_2 \quad (23)$$

The value of $\sigma_2(x)$ can be determined as stated below. In Case B, the strength of the composite is also given by $\sigma_{c,max}$ as well as in Case A. Thus in Case B, by using Equation 23 in which σ_c is taken as $\sigma_{c,max}$, the value of $\varepsilon(x)$ can be calculated in the following manner using the condition that the normal stress (load) should be equal in any cross-section.

Equation 7 can be rewritten as

$$\sigma_2(x + \Delta x) - \sigma_2(x) = \frac{1}{A_2} [\pi d_1 \tau_{1-2}(x) \Delta x + \pi d_{1+2} \tau_{2-3}(x) \Delta x] \quad (24)$$

where Δx is the differential operator of x. First we consider the situation at $x = 0$. The true strain in the x direction of the composite at $x = 0$ is equal to ε_d at which $\sigma_{c,d}$ reaches a maximum, which can be determined from Equation 22. Thus the values of $\gamma_{1-2}(0)$ and $\gamma_{2-3}(0)$ can be approximately expressed by setting $\bar{\varepsilon} = \varepsilon(x)$ in Equations 11 and 12, and by substituting $\varepsilon(x) = \varepsilon_d$ and $x = 0$ into Equations 11 and 12, respectively. Substituting $\gamma_{1-2}(0)$ and $\gamma_{2-3}(0)$ into Equation 9, we can determine $\tau_{1-2}(0)$ and $\tau_{2-3}(0)$. The value of σ_2 is zero at $x = 0$, since the Nb_3Sn is broken at $x = 0$ by definition. Thus the value of $\sigma_2(\Delta x)$ can be calculated by substituting $\tau_{1-2}(0)$, $\tau_{2-3}(0)$ and $\sigma_2(0)$ ($= 0$) into Equation 24. The value of $\varepsilon(\Delta x)$ can then be calculated by substituting $\sigma_2(\Delta x)$ into Equation 23.

In the next step, $\gamma_{1-2}(\Delta x)$ and $\gamma_{2-3}(\Delta x)$ can be calculated by substituting $\varepsilon(x) = \varepsilon(\Delta x)$ and $x = \Delta x$ into Equations 11 and 12 and then $\tau_{1-2}(\Delta x)$ and $\tau_{2-3}(\Delta x)$ from Equation 9. Substituting $\tau_{1-2}(\Delta x)$, $\tau_{2-3}(\Delta x)$ and $\sigma_2(\Delta x)$ into Equation 24, we have $\sigma_2(2\Delta x)$. Substituting $\sigma_2(2\Delta x)$ into Equation 23, we have $\varepsilon(2\Delta x)$. In this way, by increasing x step by step by Δx, the quantity $\varepsilon(\Sigma x_i)$ can be obtained. Of course, when the situations of $\gamma_{y_1} \leqq \varepsilon(x)[(l/2) - x]$ and $\gamma_{y_2} \leqq \varepsilon(x)[(l/2) - x]$ appear during this process, Equation 8 should be used for estimation of $\tau_{1-2}(x)$ and $\tau_{2-3}(x)$ instead of Equation 9. The average strain of composite $\bar{\varepsilon}$ is given by

$$\bar{\varepsilon} = \left[\sum_{i=0}^{\frac{l/2}{\Delta x} - 1} \varepsilon(i\Delta x) \Delta x \right] \Bigg/ (l/2) \quad (25)$$

4. Results of calculation

First σ_{yj}, σ_{uj} and ε_{uj} (where j refers to the layer) were measured experimentally for niobium, whose data are given by Ochiai *et al.* [1], and those for Cu–Sn were deduced by measuring the tin concentration in the Cu–Sn matrix, X_{Sn}, followed by interpolation in the σ_y–X_{Sn}, σ_u–X_{Sn} and ε_u–X_{Sn} relations for fully annealed

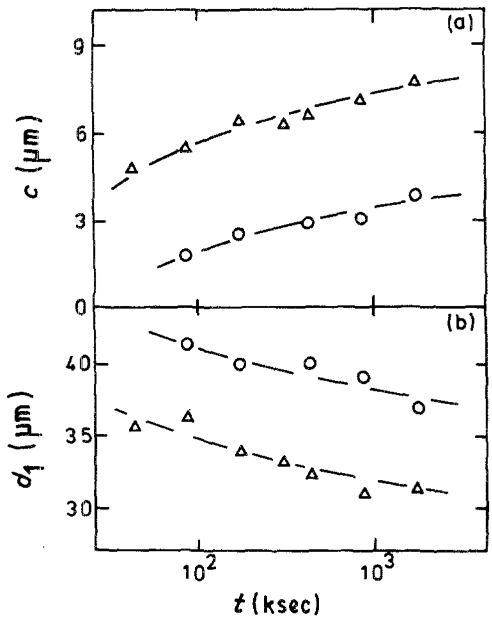

Figure 4 Variations of (a) c and (b) d_1 as a function of annealing time at the annealing temperatures of (○) 973 and (△) 1073 K.

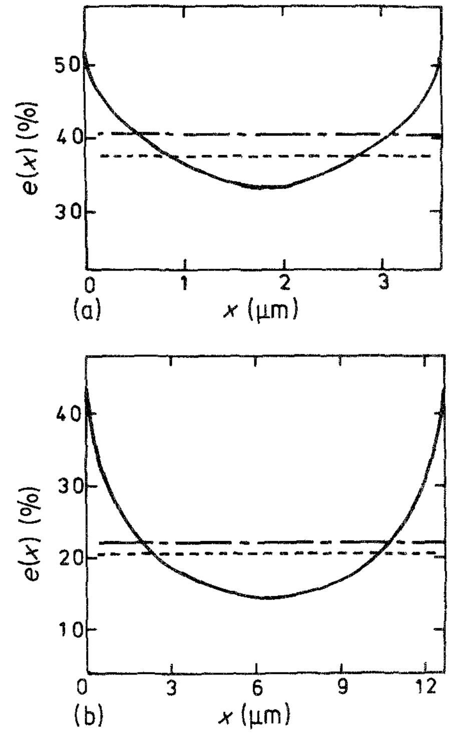

Figure 6 (——) Variation of $e(x)$ in Case B in specimens with (a) V_2 = 0.035 made by annealing at 973 K for 86 ksec and (b) V_2 = 0.145 made by annealing at 1073 K for 1730 ksec, together with the calculated values of $\bar{e}$ for (---) Case A and (- · -) Case B for comparison.

Cu–Sn alloys [15], as in our former work [1]. Those for copper were taken from the values for $X_{Sn} = 0$. The value of ε_{yj}, τ_{yj} and γ_{yj} were calculated from $\sigma_{yj}E_j$, $\sigma_{yj}/2$ and τ_{yj}/G_j, respectively. These yield and tensile stresses and strains both in tensile and shear conditions were thus determined for each heat treatment. E_1, E_3 and E_4 were taken to be 105, 125 and 125 GPa, respectively, and G_1, G_3 and G_4 to be 38, 48 and 48 GPa, respectively. Then a_j, b_j and n_j (j = 1, 3 and 4) were calculated from Equations 3 to 5. The values of l and V_1 to V_4 were taken from Ochiai *et al.* [1]. As c and d_1 varied as a function of annealing time as shown in Fig. 4, the values of d_1 and d_{1+2} ($= d_1 + 2c$) were taken from Fig. 4. The value of d_{1+2+3} was calculated to be 71.5 μm from the bronze ratio of the present specimens (= 2) and the original diameter of niobium filaments (41.3 μm). After determining these values, the values of σ_c and $\bar{e}$ (normal elongation to failure) were calculated following the methods stated in Sections 3.2 and 3.3 for Cases A and B, respectively.

Fig. 5 shows the variation of σ_c plotted against V_2. Within the range investigated, the calculated values of σ_c are nearly the same as those measured experimentally, indicating that the load-bearing capacity of the present composite is determined by the load-bearing capacity of the ductile components, as formulated in the present work.

The normal elongation $e(x)$ in Case B as a function of x for the specimen with $V_2 = 0.035$ made by annealing at 973 K for 86 ksec, and that with $V_2 = 0.145$ made by annealing at 1073 K for 1730 ksec, is shown in Fig. 6, where the average elongations $\bar{e}$ for Cases A and B calculated by the present method are superimposed for comparison. The value of $e(x)$ for Case B decreases with increasing x up to $x = l/2$, at which it becomes a minimum. It is evident that the elongation of ductile components is supressed by the existence of Nb_3Sn segments in Case B. On the other hand, $\bar{e}$ is independent of x by definition in Case A.

Fig. 7 shows the ratio of the load carried by the Nb_3Sn compound, $\bar{\sigma}_2 V_2$, to the total stress of the

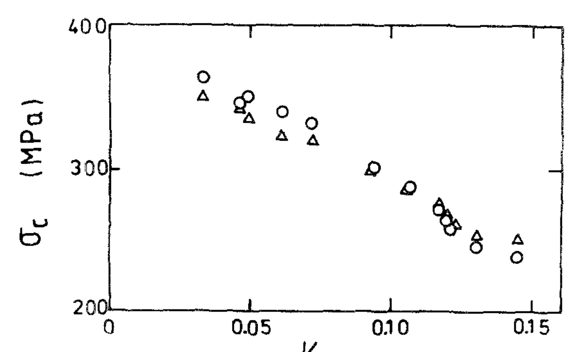

Figure 5 Comparison of (○) calculated with (△) experimental values of σ_c.

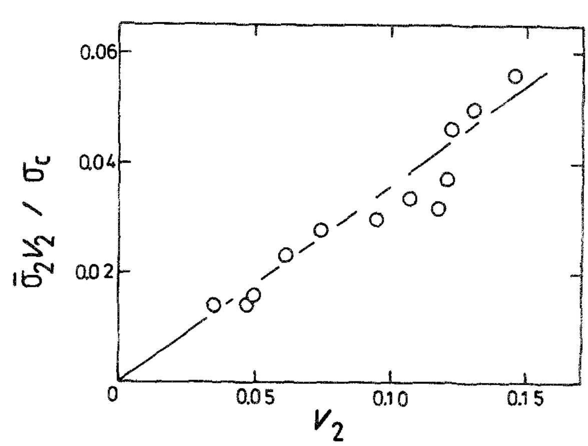

Figure 7 Increase in $\bar{\sigma}_2 V_2/\sigma_c$ with increasing V_2 in Case A.

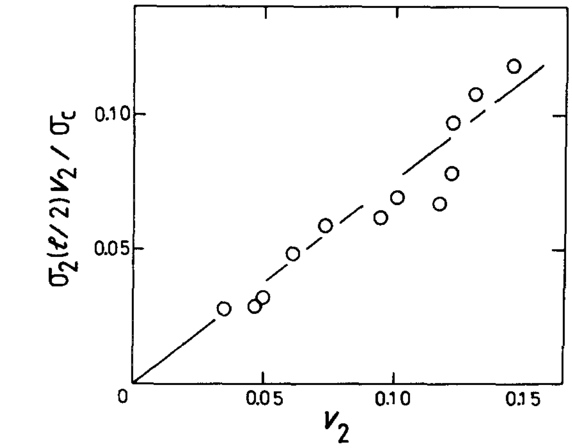

Figure 8 Increase in $\sigma_2(l/2)V_2/\sigma_c$ with increasing V_2 in Case B.

composite at fracture for Case A. The ratio $\bar{\sigma}_2 V_2/\sigma_c$ increases with increasing V_2, indicating that the existence of segmented Nb_3Sn compound reduces elongation of the composite with increasing V_2 when Equation 6 is obeyed. In Case B, the ratio of the load carried by Nb_3Sn segments to the stress of the composite increases with increasing x and it becomes a maximum at $x = l/2$. Fig. 8 shows the variation of $\sigma_2(l/2)V_2/\sigma_c$ in Case B as an example. The ratio increases with increasing V_2, indicating that the elongation of the composite is also reduced with increasing V_2 when V_2 becomes large, when Equations 23 and 25 are obeyed.

The calculated normal strain to failure of composite, $\bar{e}$, is presented in Figs 9 and 10 for Cases A and B, respectively, where the measured values of $\bar{e}$ are superimposed for comparison. The tendency that $\bar{e}$ decreases with increasing V_2 is well realized by the present calculation method, although some discrepancy between measured and calculated values is found for large V_2. The reason why such a discrepancy arises might be attributed to the many approximations made in the present calculation. Although the present calculation results do not agree with experimental results in a rigid manner, it might be concluded that the present approximate calculation method is useful at least to predict $\bar{e}$ in a qualitative manner.

In the present work, the difference in $\bar{e}$ between Cases A and B was small within the accuracy of the present calculation methods. Therefore it was not determined which of Cases A and B is the more realistic. On this point further study is needed.

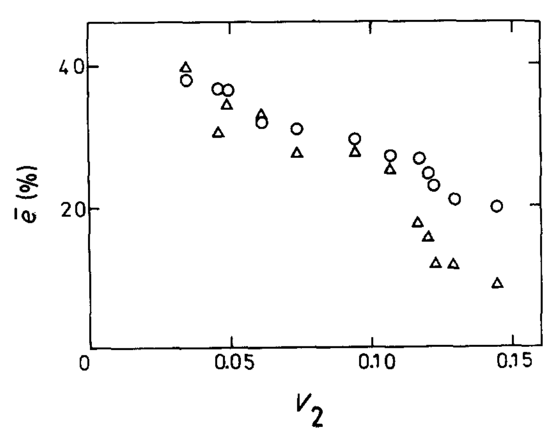

Figure 9 Comparison of (○) calculated and (△) experimental values of $\bar{e}$ in Case A.

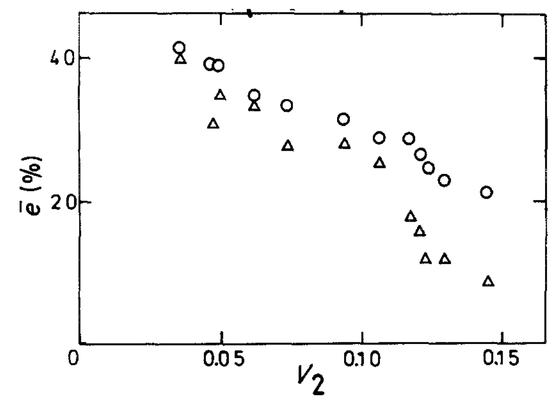

Figure 10 Comparison of (○) calculated and (△) experimental values of $\bar{e}$ in Case B.

5. Conclusions

Approximate calculation methods based on shear lag analysis and the plastic instability approach for metallic composites were proposed to describe the tensile strength and elongation to failure of multifilamentary Nb_3Sn superconducting composite materials with small amounts of Nb_3Sn compound which shows multiple fracture under loading. The application of the proposed methods to the experimental results showed that the proposed methods can fairly well describe the results.

Acknowledgements

The authors wish to express their gratitude to Messrs T. Unesaki and I. Nakagawa at Kyoto University for their help in EPMA and SEM studies. They also express their gratitude to the Ministry of Education, Science and Culture of Japan for a grant-in-aid for energy research (No. 61050033).

References

1. S. OCHIAI, K. OSAMURA and T. UEHARA, *J. Mater. Sci.* **21** (1986) 1027.
2. A. KELLY and W. R. TYSON, *J. Mech. Phys. Solids* **13** (1965) 329.
3. C. ZWEBEN and B. W. ROSEN, *ibid.* **18** (1970) 189.
4. C. ZWEBEN, *Eng. Frac. Mech.* **6** (1974) 1.
5. M. A. WRIGHT and J. L. WILLS, *J. Mech. Phys. Solids* **22** (1974) 161.
6. W. H. HERRING, J. L. LYTTON and J. H. STEELE Jr, *Met. Trans.* **4** (1973) 807.
7. O. OKUNO and I. MIURA, *J. Jpn Inst. Metals* **42** (1978) 736.
8. B. W. ROSEN, *AIAA J.* **2** (1964) 1985.
9. S. OCHIAI, K. OSAMURA and K. ABE, *Z. Metallkde* **76** (1985) 402.
10. S. OCHIAI and K. OSAMURA, *ibid.* **76** (1985) 485.
11. N. F. DOW, GEC Missile and Space Division, Report No. R63SD61, quoted by G. S. Holister and C. Thomas in "Fibre Reinforced Materials" (Elsevier, London, 1966) p. 23.
12. S. T. MILEIKO, *J. Mater. Sci.* **4** (1969) 974.
13. G. GARMONG and R. B. THOMPSON, *Met. Trans.* **4** (1973) 863.
14. S. OCHIAI and Y. MURAKAMI, *J. Mater. Sci.* **15** (1980) 1798.
15. ASM Committee on Copper and Copper Alloys: Metals Handbook, Vol. 2 ASM, Metals Park, Ohio, 1979) p. 275.

Received 4 August
and accepted 22 September 1986